Am J Physiol Lung Cell Mol Physiol 299: L711–L719, 2010.
First published September 10, 2010; doi:10.1152/ajplung.00072.2010.

Preexposure to hyperoxia causes increased lung injury and epithelial apoptosis in mice ventilated with high tidal volumes

Patrudu S. Makena,[1] Charlean L. Luellen,[1] Louisa Balazs,[3] Manik C. Ghosh,[2] Kaushik Parthasarathi,[2,4] Christopher M. Waters,[1,2] and Scott E. Sinclair[1,2]

Departments of [1]Medicine, [2]Physiology, [3]Pathology, and [4]Biomedical Engineering and Imaging, University of Tennessee Health Science Center, Memphis, Tennessee

Submitted 3 March 2010; accepted in final form 6 September 2010

Makena PS, Luellen CL, Balazs L, Ghosh MC, Parthasarathi K, Waters CM, Sinclair SE. Preexposure to hyperoxia causes increased lung injury and epithelial apoptosis in mice ventilated with high tidal volumes. *Am J Physiol Lung Cell Mol Physiol* 299: L711–L719, 2010. First published September 10, 2010; doi:10.1152/ajplung.00072.2010.—Both high tidal volume mechanical ventilation (HV) and hyperoxia (HO) have been implicated in ventilator-induced lung injury. However, patients with acute lung injury are often exposed to HO before the application of mechanical ventilation. The potential priming of the lungs for subsequent injury by exposure to HO has not been extensively studied. We provide evidence that HO (90%) for 12 h followed by HV (25 μl/g) combined with HO for 2 or 4 h (HO-12h+HVHO-2h or -4h) induced severe lung injury in mice. Analysis of lung homogenates showed that lung injury was associated with cleavage of executioner caspases, caspases-3 and -7, and their downstream substrate poly(ADP-ribose) polymerase-1 (PARP-1). No significant lung injury or caspase cleavage was seen with either HO for 16 h or HV for up to 4 h. Ventilation for 4 h with HO (HVHO) did not cause significant lung injury without preexposure to HO. Twelve-hour HO followed by lower tidal volume (6 μl/g) mechanical ventilation failed to produce significant injury or caspase cleavage. We also evaluated the initiator caspases, caspases-8 and -9, to determine whether the death receptor or mitochondrial-mediated pathways were involved. Caspase-9 cleavage was observed in HO-12h+HVHO-2h and -4h as well as HO for 16 h. Caspase-8 activation was observed only in HO-12h+HVHO-4h, indicating the involvement of both pathways. Immunohistochemistry and in vitro stretch studies showed caspase cleavage in alveolar epithelial cells. In conclusion, preexposure to HO followed by HV produced severe lung injury associated with alveolar epithelial cell apoptosis.

mechanical ventilation; mouse

DESPITE ADVANCEMENT IN CRITICAL care, acute lung injury (ALI) and the acute respiratory distress syndrome (ARDS) continue to affect ~200,000 patients in the United States annually, with an associated mortality rate between 30 and 60% (23). ALI/ARDS is characterized by noncardiogenic pulmonary edema, altered lung mechanics and gas exchange, and local and systemic inflammation. The resulting hypoxemic respiratory failure requires the use of mechanical ventilation with high levels of oxygen to maintain adequate oxygen delivery to vital organs. Although a potentially life-saving intervention, mechanical ventilation can also cause additional lung damage known as ventilator-induced lung injury (VILI). Several potential mechanisms have been postulated to produce VILI, the best studied of which is lung overdistention due to excessively large tidal volumes (17). A large, randomized, clinical trial has shown that mortality was reduced when patients were ventilated with lower tidal volumes, presumably due to decreased overdistention and less VILI (1).

Prolonged exposure to hyperoxia (HO) in the absence of mechanical ventilation can also cause lung injury with histopathological changes similar to that seen in ARDS (2, 19, 20). Both apoptosis and necrosis have been described in alveolar epithelial cells during prolonged HO (15). In the first 3 intensive care unit days, most ARDS patients are ventilated with a mean fraction of inspired oxygen ($F_{I_{O_2}}$) > 59% (mean $F_{I_{O_2}}$ delivered on *day 1* = 70%) (9), but the most severely ill often require much higher $F_{I_{O_2}}$ (100%) for prolonged periods or frequent intervals (6). However, despite their ubiquitous concomitant use, the combined effects of mechanical ventilation and HO have not been extensively studied. Several recent reports have confirmed that the combination of large tidal volume ventilation (HV) with HO produces lung injury faster and more severe than either insult alone (3, 5, 8, 13, 14, 22). In addition to HO during mechanical ventilation, patients with evolving ALI are frequently exposed to high $F_{I_{O_2}}$ before initiation of mechanical ventilation. Several animal studies have shown that prolonged (24–48 h) HO exposure before mechanical ventilation produced increased lung injury compared with mechanical ventilation alone, suggesting that this O_2 preexposure may make the lung more vulnerable to VILI (3, 8). The mechanism(s) by which these combined insults produce increased lung injury remain uncertain. We hypothesized that preexposure to a relatively short (12-h) period of HO before initiation of mechanical ventilation would increase the severity of lung injury. We additionally hypothesized that this injury would be associated with increased cell death via caspase-mediated apoptosis in the alveolar epithelium.

MATERIALS AND METHODS

Animals. Male C57BL/6J mice aged 8–10 wk (26–30 g body wt) were obtained from Charles River Laboratories (Wilmington, MA). All animals received care in accordance with the *Guide for the Care and Use of Laboratory Animals* (NIH Publication No. 86-23). The animal care and use committees of the University of Tennessee Health Science Center (UTHSC) approved the study.

Experimental conditions. Mice were divided into nine groups (Table 1): spontaneously breathing with normoxia (SVNO; $F_{I_{O_2}}$ = 0.21); spontaneously breathing with HO (SVHO; $F_{I_{O_2}}$ = 0.9 for 4 and 16 h); HV with normoxia [HVNO; 25 μl/g tidal volume at respiration rate (RR) of 60 breaths/min for 2 or 4 h]; and HV with HO for 4 h before (HVHO) and after 12-h preexposure to HO (12h+HVHO-2h or -4h). A separate group was subjected to 4 h of low tidal volume ventilation (6 μl/g tidal volume) with HO after 12-h preexposure to

Address for reprint requests and other correspondence: S. E. Sinclair, Dept. of Medicine, Univ. of Tennessee Health Science Center, 956 Court Ave. Rm. E222a, Memphis, TN 38163 (e-mail: ssincla1@uthsc.edu).

Table 1. *Summary of experimental groups*

Conditions	Treatment	Time
SVNO	Spontaneously breathing (SV) with normoxia (NO)	
HVNO-2h	High tidal volume mechanical ventilation (HV) with NO	2 h (HV)
HVNO-4h	HV with NO	4 h (HV)
SVHO-4h	SV with hyperoxia (HO)	4 h (HO)
SVHO-16h	SV with HO	16 h (HO)
HVHO-4h	HO in combination with HV	4 h (HV + HO)
12h-HO+HVHO-2h	Preexposure to HO for 12 h followed by HV with HO for 2 h	12 h (HO) +2 h (HV + HO)
12h-HO+HVHO-4h	Preexposure to HO for 12 h followed by HV with HO for 4 h	12 h (HO) +4 h (HV + HO)
12h-HO+LVHO-4h	Preexposure to HO for 12 h followed by low tidal volume mechanical ventilation with HO for 4 h	12 h (HO) +4 h (LV + HO)

HV, 25 μl/g; HO, 90% Fi_{O_2}.

HO (12h+LVHO-4h). Positive end-expiratory pressure (PEEP) was set at 0 for all mechanically ventilated animals.

Ventilation protocol. Mice were anesthetized by intraperitoneal injection of ketamine/xylazine (1:1, 0.15 ml/10 g). A tracheotomy was performed using an 18-gauge needle, and mice were ventilated via a mouse ventilator (Ugo Basile, Comario, Italy). Tidal volume and RR were calculated according to body weight and experimental condition. End-tidal CO_2 was measured at *time 0* and every 30 min thereafter (Micro-CapnoGraph CI240; Columbus Instruments, Columbus, OH). Inspiratory gas mixture was maintained using a precision gas mixer (PEGAS 4000MF; Columbus Instruments). Pulse, heart rate, and arterial oxygen saturation were monitored using a small animal oximeter (Mouse OX; STARR Life Sciences) and recorded at *time 0* and every 30 min thereafter. A catheter was placed in the peritoneal cavity for crystalloid administration (100 μl of 0.9% NaCl at *time 0* and every 1 h thereafter). Adequate anesthesia was maintained with inhalation of 1% isoflurane. Rectal temperature was maintained within the normal range with a heat lamp.

Assessment of lung injury: respiratory system compliance. Quasi-static compliance (Cst) was estimated at *time 0* and at the end of mechanical ventilation by fitting data derived from a pressure-volume loop to the Salazar-Knowles equation (24). Measurements and calculations were performed using a flexiVent system (SCIREQ, Chandler, AZ).

Bronchoalveolar lavage fluid protein concentration. At the end of the experiment, the lungs were lavaged three times with 1.0-ml aliquots of PBS with 0.6 mM EDTA at 37°C, and the recovered fluid volume was recorded. The bronchoalveolar lavage fluid (BALF) was centrifuged at 14,000 *g* for 5 min at 4°C, and cell-free supernatant was removed and stored in aliquots at −80°C. Total protein was measured with the Bradford assay.

Lung histology. At the end of the experiment, the lungs were removed and perfused with 5 ml of 1 M PBS containing 100 units of heparin to remove red blood cells. The right lung of each animal was fixed with intratracheal instillation of 10% buffered formalin at ~20 cmH_2O. Fixed lungs were embedded in paraffin, cut into 4-μm sections, and stained with hematoxylin and eosin (H&E) in a histology lab (Dept. of Pathology, UTHSC). H&E-stained lung sections ($n = 4$ per condition) were scored by a pathologist blinded to the experimental condition. In each section, 10 fields were randomly scored for *1*) interstitial edema, *2*) alveolar edema, *3*) hemorrhage, and *4*) neutrophil infiltrates at ×40 magnification under microscope and digitized slides. The scores from each field were averaged and presented on a scale of 0–4 (0 being none present, and 4 being severe and diffuse throughout the chosen field). The histological composite scores (Fig. 2) represent the sum of the mean injury subtype scores for each condition on a scale of 0–16 (25).

Cell culture. Mouse alveolar epithelial MLE-12 cells [American Type Culture Collection (ATCC), Manassas, VA] were cultured in DMEM (GIBCO, Carlsbad, CA) supplemented with 10% FBS (Cellgro, Herndon, VA, or GIBCO). Cells were cultured until 85–100% confluence on BioFlex plates coated with collagen type I (Flexcell International, Hillsborough, NC).

Cyclic mechanical strain. Cyclic strain was performed on MLE-12 cells using a Flexcell FX-4000 Tension Plus Strain Unit (Flexcell International). Cell monolayers were exposed to either room air or HO (90% O_2 and 5% CO_2) in a contained chamber for 12 h followed by 4 h of cyclic strain in either room air or HO depending on the condition. MLE-12 cells were stretched at either 20% (HV) or 6% (low tidal volume) elongation at 30 cycles/min (cpm).

Immunoblot (Western) analysis. The left lung of each mouse was removed and homogenized (OMNI TH tissue homogenizer; OMNI International) with 3 ml of lung lysis buffer [50 mM Tris (pH 7.4), 4 mM KCl, 1% Nonidet P-40 (vol/vol), 0.25% sodium deoxycholate, 150 mM NaCl, 1 mM EGTA, 1 mM phenylmethylsulfonyl fluoride, 10 μg/ml leupeptin, 0.2 U/ml aprotinin, 1 μg/ml pepstatin, 1 mM Na_3VO_4, 1 mM NaF] and sonicated for 10 s [20 pulses; Omni Sonic Ruptor 250 Watt Ultrasonic Homogenizer (OR250); OMNI International] (4).

For the in vitro experiments, MLE-12 cells were lysed on ice using RIPA buffer (50 mM Tris·HCl, pH 7.4, 150 mM NaCl, 2 mM EDTA, 1% Nonidet P-40, 0.1% SDS) with protease inhibitor cocktail (Roche). Lysates were centrifuged at 4°C and 16,000 *g* for 15 min, and total protein was measured (BCA assay; Pierce, Rockford, IL). Twenty micrograms of each protein sample were mixed with 10 μl of 3× SDS loading buffer, boiled at 70°C for 10 min, and loaded on NuPAGE 4–12% Bis-Tris gel (Invitrogen, Carlsbad, CA). Immunoblotting was performed on 0.25-μm nitrocellulose membrane (Bio-Rad) at 170-mA start and 110-mA end at 30 V for 1 h in NuPAGE9 transfer buffer (Invitrogen) containing 20% methanol. Membranes were blocked in 5% nonfat dry milk in Tris-buffered saline (Bio-Rad) containing 0.1% Tween 20 for 1 h at 37°C. Primary antibodies mouse anti-procaspase and cleaved caspases-3, -7, -8, and -9, poly(ADP-ribose) polymerase (PARP), and GAPDH were obtained from Cell Signaling Technology (Danvers, MA) and incubated overnight at 4°C. Proteins were visualized with horseradish peroxidase (HRP)-coupled anti-rabbit IgG secondary antibody (Cell Signaling Technology) and luminol chemiluminescent substrate LumiGLO (Cell Signaling Technology). Densitometry analysis was performed with ImageJ 1.42 image processing software (W. S. Rasband, National Institutes of Health, Bethesda, MD; http://rsbweb.nih.gov/ij/) using gel analysis method.

Immunohistochemistry. Immunohistochemistry was performed according to the manufacturer's protocol using anti-cleaved caspases-3 (Biocare Medical) in a histology lab (Dept. of Pathology, UTHSC) using BenchMark XT/LT automated slide-staining system (7).

Tissue immunofluorescence and confocal microscopy. Lung tissue immunofluorescence was performed as previously described (21). Lung sections were incubated overnight in a moist chamber with 200 μl of 1:100 anti-cleaved PARP-1 (Asp214) antibody (murine specific; Cell Signaling Technology). The primary antibody was removed and washed 3 times with PBST (0.01% Tween 20 in PBS) and incubated

with 200 μl of 2 μg/ml secondary antibody conjugated with Alexa Fluor 488 (Invitrogen) for 1 h. Slides were mounted with Vectashield and stored at −20°C in the dark. Confocal images were obtained 48 h later using a Bio-Rad (Hercules, CA) MRC 1024 imaging system attached to a BX50 (Olympus, Downingtown, PA) microscope. Fluorophores were excited using the 488-nm line of a krypton-argon laser. Emitted fluorescence was collected using a ×60 objective lens (NA 1.4 Oil), and the images were recorded using LaserSharp 2000 software (Bio-Rad).

Statistical analysis. All values are expressed as means ± SD unless otherwise stated. ANOVA was used to compare mean values for the different groups followed by Scheffé test for multiple comparisons between groups, with significance set at $P < 0.05$. Nonparametric data were analyzed using the Kruskal-Wallis one-way ANOVA on ranks with post hoc pairwise comparisons made using the Holm-Sidak method. All statistics were performed using SigmaStat 3.5 software.

RESULTS

HV and HO following pretreatment with HO caused severe lung injury. We compared the extent of lung injury in 9 different groups (Table 1) by assessment of histological evidence of lung injury as well as Cst and BALF protein concentration. Figure 1 shows representative photomicrographs of lung sections from each group, and Fig. 2, *left*, shows a comparison of the lung injury scores (LIS). Figure 1*A* shows normal lung parenchyma from control mice (SVNO). Figure 1*B* shows some intraalveolar edema (↑) and minimal neutrophil infiltration (←) in mice exposed to HVNO for 2 h, whereas in Figure 1*C* animals exposed to HVNO for 4 h exhibit foci of intraalveolar hemorrhage (▲) and neutrophil infiltration. In Figure 1, *D* and *E*, mice exposed to SVHO for 4 or 16 h, respectively, developed mild intraalveolar edema and neutrophil infiltration. When ventilated with high tidal volumes and HO (HVHO) for 4 h, mice exhibited minimal edema along with mild intraalveolar hemorrhage and neutrophil infiltration (Fig. 1*F*). In contrast to these groups, animals subjected to 12-h preexposure to HO followed by mechanical ventilation (HVHO) for 2 h (Fig. 1*G*) developed diffuse interstitial hemorrhage, edema, and neutrophil infiltration. When the ventilation period was extended to 4 h following HO preexposure, the observed intraalveolar and interstitial hemorrhage, edema, and neutrophil infiltration was at its most severe and diffuse (Fig. 1*H*) among the experimental groups studied. When 12-h HO preexposure was followed by 4 h of low tidal volume ventilation (Fig. 1*I*), only mild intraalveolar edema and neutrophil infiltration were seen.

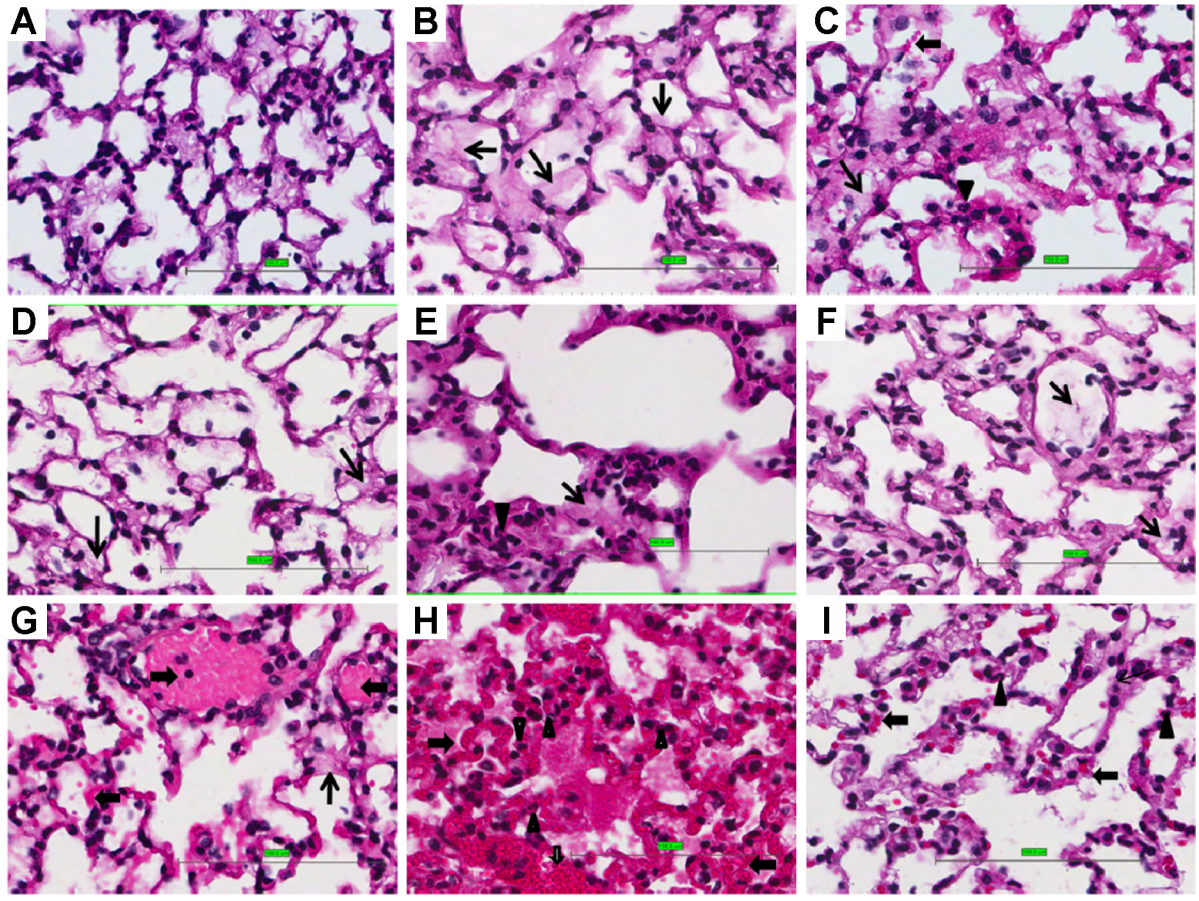

Fig. 1. Preexposure to hyperoxia (HO) followed by high tidal volume mechanical ventilation (HV) with HO caused lung injury. $n = 4$ Mice per group. Hematoxylin-eosin (H&E)-stained, formalin-fixed, paraffin-embedded lung tissues from mice, subjected to spontaneously breathing with normoxia (SVNO; *A*), HV with 2-h normoxia (HVNO-2h; *B*), HVNO-4h (*C*), SVHO-4h (*D*), SVHO-16h (*E*), HVHO-4h (*F*), HO for 12 h followed by HV combined with HO for 2 h (12h-HO+HVHO-2h; *G*), 12h-HO+HVHO-4h (*H*), low tidal volume ventilation with HO for 4 h after 12-h preexposure to HO (12h-HO+LVHO-4h; *I*), 12h-HO+HVHO-2h (*G*), and 12h-HO+HVHO-4h (*H*) conditions show evidence of extensive lung injury with interstitial and alveolar edema (↑), hemorrhage (←), and acute inflammatory cell infiltration (▲) compared with other experimental conditions (scale: 100 μm).

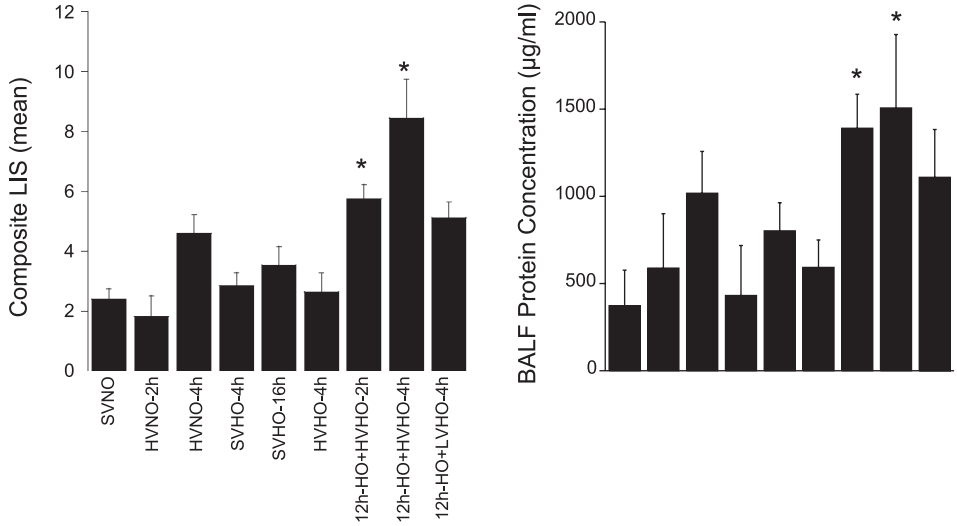

Fig. 2. The composite lung injury scores (LIS; *left*) represent the sum of the mean injury subtype scores for each condition on a scale of 0–16 ($n = 4$ mice per group). The LIS were significantly higher in animals preexposed to HO for 12 h followed by 2 and 4 h of HV and HO ($P < 0.05$). No other condition showed statistically significant increases in lung injury compared with controls (SVNO). *$P < 0.05$ compared with SVNO. Bronchoalveolar lavage fluid (BALF) protein concentrations (*right*) mirror the LIS ($n = 3$ mice per group).

Although injury was observed in some categories for animals treated with HO alone or MV alone, the composite LIS ($n = 4$ mice per group) was significantly different only in the two conditions in which mice were preexposed to 12 h of HO followed by HV (12h-HO+HVHO-2h and -4h) compared with controls (SVNO). BALF protein concentrations (Fig. 2, *right*) mirror the LIS in that the more severe the LIS, the higher the mean protein concentration. Lung mechanics (Fig. 3) were stable in all experimental conditions except when preexposure to HO was followed by HVHO for 2 or 4 h, when the Cst at the end of the experiment decreased compared with *time 0*. This only reached statistical significance in the 12h-HO+HVHO-4h group ($n = 3$ mice per group).

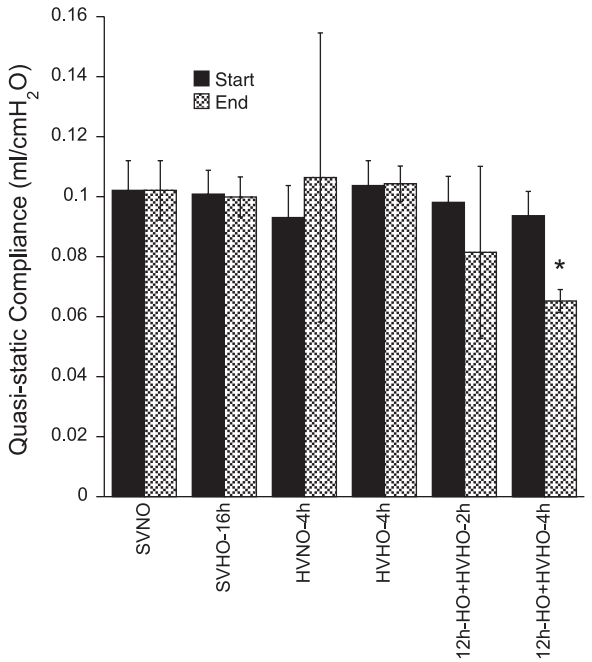

Fig. 3. Quasi-static thoracic compliance for selected experimental conditions at *time 0* and at the end of the experiment. All measurements remained stable except in the 12h-HO+HVHO-2h and 12h-HO+HVHO-4h conditions where the compliance decreased. *$P < 0.05$ compared with same condition at *time 0* and with SVNO.

HV and HO following pretreatment with HO activated executioner caspases (caspase-3 and caspase-7) and PARP-1. To test the hypothesis that apoptosis was associated with lung injury due to combined HV and HO, we evaluated the cleavage of executioner caspases-3 and -7 and their substrate PARP-1 in all experimental conditions. PARP-1 is a nuclear enzyme involved in DNA repair, DNA stability, and transcriptional regulation, which catalyzes covalent attachment of long, branched chains of poly(ADP-ribose) and is a target for cleavage by caspases (12). Consistent with histological data, neither HO nor HV alone caused cleavage of caspase-3, caspase-7, or PARP-1 (Fig. 4). However, pretreatment with HO for 12 h followed by HV (12h-HO+HVHO-2h and -4h) caused cleavage of both caspase-3 and -7 as well as PARP-1. Pretreatment with HO followed by low tidal volume ventilation did not cause caspase or PARP-1 cleavage.

HV and HO following pretreatment with HO activated initiator caspases, caspases-8 and -9. We further examined the activation of caspases-8 and -9 to understand whether the apoptotic signal originated either from the death receptor or mitochondrial pathway. As shown in Fig. 5, immunoblot data from whole lung homogenates demonstrated that both caspase-8 and -9 were upregulated in the 12h-HO+HVHO-2h and -4h groups. Cleaved caspase-9 was more abundant in 12h-HO+HVHO-2h, indicating that both pathways were activated in these conditions, but the signal decreased after 2 additional hours of ventilation. Caspase-9 was also cleaved following 16 h of SVHO. No other conditions produced caspase-8 or -9 cleavage.

HV following pretreatment with HO showed cleaved caspase-3 activation in lung epithelial cells. To localize cleaved caspase-3 in lung tissues, we performed immunohistochemistry using anti-cleaved caspase-3 and immunofluorescence using antibodies to cleaved PARP-1 in SVNO and 12h-HO+HVHO-4h conditions to determine the cell types that were actively undergoing apoptosis. Figure 6 shows that alveolar epithelial cells stained positive for both cleaved caspase-3 in mice exposed to 12h-HO+HVHO-4h. Positive staining was consistently seen in airway and alveolar epithelial cells, but apoptosis in other cell types (e.g., endothelial or immune cells) cannot be excluded. No positive staining was seen in control lungs.

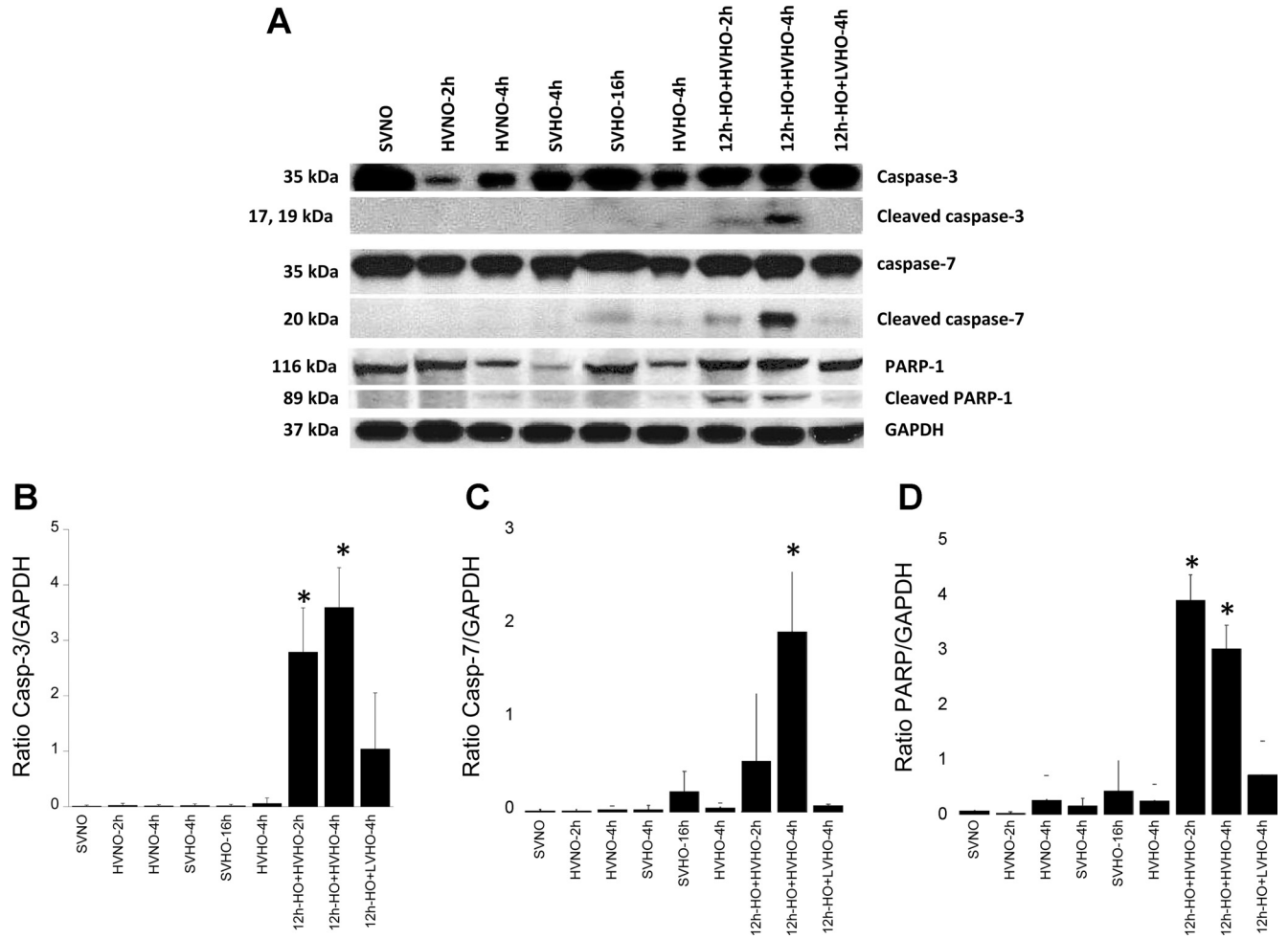

Fig. 4. *A*: activation of executioner caspases (caspases-3 and -7) and their downstream substrate, poly(ADP-ribose) polymerase-1 (PARP-1), in whole lung homogenates of mice subjected to SVNO (*lane 1*), HVNO-2h (*lane 2*), HVNO-4h (*lane 3*), SVHO-4h (*lane 4*), SVHO-16h (*lane 5*), HVHO-4h (*lane 6*), 12h-HO+HVHO-2h (*lane 7*), 12h-HO+HVHO-4h (*lane 8*), and 12h-HO+LVHO-4h (*lane 9*). *B*, *C*, and *D* show densitometry for caspase-3 (Casp-3), caspase-7, and PARP-1, respectively. Caspase and PARP-1 cleavage were observed only in 12h-HO+HVHO-2h and -4h. No significant caspase cleavage was observed in any other condition. Blots shown are representative from 3 different animals per group. *$P < 0.05$ compared with SVNO.

Cyclic mechanical strain following pretreatment with HO promotes cleavage of caspases-3 and -7 and PARP-1 in mouse alveolar epithelial cell line (MLE-12 cells). To determine whether preexposure to HO followed by mechanical stretch would directly initiate apoptosis in alveolar epithelial cells, we applied cyclic mechanical strain to the mouse alveolar epithelial cell line (MLE-12) following 12-h preexposure to either room air or HO and measured activation of executioner caspases and PARP-1 cleavage using Western blot analysis of cell lysates. As shown in Fig. 7, cells exposed to normoxia without stretch (SVNO) demonstrated no cleavage of caspase-3 (Fig. 7*A*), caspase-7 (Fig. 7*B*), or PARP-1 (Fig. 7*C*). Differences in caspase-3 and caspase-7 cleavage only reached statistical significance in cells exposed to HO for 12 h followed by 4 h of 20% cyclic strain with HO (12h-HO+HVHO-4h). PARP-1 cleavage was observed in nearly all treatment groups but reached statistical significance only in the 12h-HO+HVHO-4h and HVNO-4h groups. Additionally, preexposure to 12-h HO followed by low (6%) stretch (12h-HO+LVHO-4h) did not produce significant cleavage of caspase-3, caspase-7, or PARP-1.

DISCUSSION

The unique findings of this study are: *1*) exposure to HO before initiation of HV increases susceptibility to VILI; *2*) lung injury observed in this model was associated with caspase-mediated apoptosis; and *3*) immunohistochemistry and in vitro stretch studies indicate that the apoptotic cell death pathways were activated in the alveolar epithelium.

Previous studies have demonstrated that the combination of HO and mechanical ventilation can induce lung injury. Davis et al. (5) showed that HV with 100% $F_{I_{O_2}}$ produced severe lung injury after 24 and 48 h in neonatal piglets compared with nonventilated controls. Bailey et al. (3) subjected mice to >90% $F_{I_{O_2}}$ and then to short-term (2-h) HV in the absence of PEEP. They, too, found that preexposure to HO augmented stretch-induced lung injury. However, they subjected animals to 48 h of HO, four times the length of exposure used in the current study, and then ventilated isolated ex vivo lung preparations. In the current study, all experiments were conducted in intact animals. Ehlert et al. (8) reported that lung inflammation was exacerbated when 20 ml/kg tidal volume mechanical

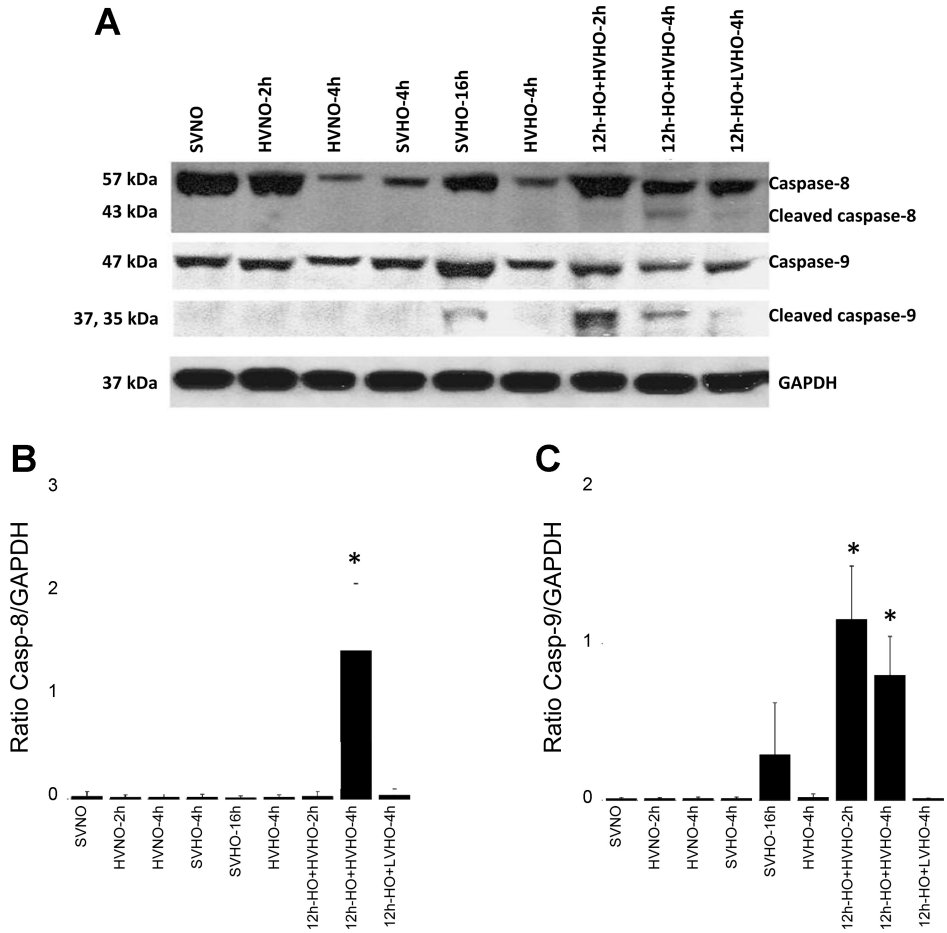

Fig. 5. *A*: activation of initiator caspases (caspases-8 and -9) in whole lung homogenates of mice subjected to SVNO (*lane 1*), HVNO-2h (*lane 2*), HVNO-4h (*lane 3*), SVHO-4h (*lane 4*), SVHO-16h (*lane 5*), HVHO-4h (*lane 6*), 12h-HO+HVHO-2h (*lane 7*), 12h-HO+HVHO-4h (*lane 8*), and 12h-HO+LVHO-4h (*lane 9*). *B* and *C* show densitometry for caspase-8 and caspase-9, respectively. Both the initiator caspases were activated in 12h-HO+HVHO-2h and -4h conditions, whereas an increase in cleaved caspase-9 was observed in SVHO-16h. No other conditions produced cleavage of either initiator caspase. Blots shown are representative from 3 different animals per group. $*P < 0.05$ compared with SVNO.

ventilation followed exposure to 3 days of $FI_{O_2} = 1.0$ in newborn piglets. In the current study, 12-h HO preexposure was employed, a time period that alone does not produce significant lung injury. Species differences between these studies also make direct comparisons difficult.

Quinn et al. (22) found that rats mechanically ventilated with 20 ml/kg tidal volumes exhibited increased lung injury when concomitantly exposed to HO. This differs from the current study in that no preexposure to HO was performed and in the species studied. This same group recently reported that the addition of HO to HV augmented lung injury in mice (14). As in the previous rat study, these mice were not exposed to HO before mechanical ventilation. Li et al. (13) found that whereas the addition of HO to high tidal volume (30 ml/kg) augmented lung injury in mice, those animals ventilated with large tidal volumes had evidence of apoptosis [TdT-mediated dUTP nick end labeling (TUNEL) and EM (electron microscopy)] regardless of exposure to room air or HO. This contrasts with the current study where only 12h-HO+HVHO-2h and -4h conditions produced activation of apoptotic pathways. These differences may be accounted for by the different methods used to measure apoptosis between the two studies, namely they may have seen caspase-independent apoptosis in conditions where we did not see caspase cleavage. Additionally, their use of larger tidal volume (30 vs. 25 ml/kg) may account for the observed differences.

Several studies have previously shown that cell death and apoptosis can result from stretching alveolar epithelial cells in vitro. Tschumperlin and Margulies (26) subjected primary isolated rat type II alveolar cells to varying degrees of stretch. They found that cell death increased with magnitude of stretch and decreased with increasing time in culture. Hammerschmidt et al. (10) subjected rat alveolar type II cells to two different stretch amplitudes (13 and 30% change in surface area) and frequencies (40 and 60 cpm). Higher frequency and larger amplitude stretch produced increased necrosis at 12, 18, and 24 h. Apoptosis was increased by higher frequency stretch at 24 h and by larger amplitude stretch at 18 and 24 h. A statistically significant increase in caspase-8 activity was observed only with large amplitude stretch for 24 h. The differences between our results and these are likely due to several factors. First, these studies used primary rat alveolar type II cells so there may be species differences compared with mice. Second, the manipulations required to isolate, culture, and prepare cells for analysis may have caused, or made the cells more susceptible to, cell death. Third, we used a cell line (MLE-12) derived from lung tumors from a mouse transgenic for simian virus 40 (SV40) large T cell antigen and thus may be less prone to apoptosis. Fourth, although the amplitude of linear deformation used in the current study is similar to those used previously (6% elongation $\approx$ 12% change in surface area; 20% elongation $\approx$ 44% change in surface area), we used a lower frequency (30 vs. 40 and 60 cpm) and shorter time period (4 vs. up to 24 h), which may have been insufficient to produce apoptosis in the absence of preexposure to HO. Alternatively, the protocol employed by Hammerschmidt et al. (10) may have produced

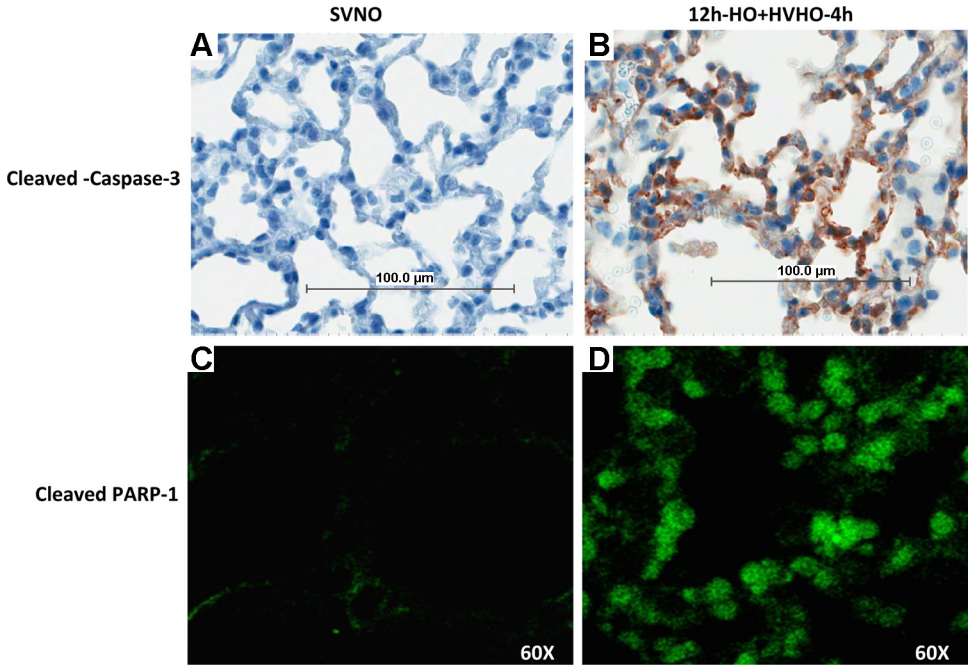

Fig. 6. Immunohistochemistry of cleaved caspase-3 in control SVNO mice (*A*) and mice exposed to 12h-HO+HVHO-4h (*B*). Confocal imaging of immunofluorescence staining for cleaved PARP-1 in mouse lungs subjected to SVNO (*C*) and to 12h-HO+HVHO-4h (*D*). SVNO produced no significant positive staining for either cleaved caspase-3 or cleaved PARP-1, whereas epithelial cells stained positive for both cleaved caspase-3 and cleaved PARP-1 antibodies after exposure to 12h-HO+HVHO-4h (n = 3 animals per group). Representative images from a single animal are shown in 100-μm scale.

additional non-caspase-mediated cell death that was not detected by our methods. Finally, neither of these nor, to our knowledge, any other reported studies have looked at combined HO and stretch in vitro.

Potential shortcomings of the experimental model. This model is designed to determine the roles of HO, mechanical stretch, and the combination of these two insults in the development of VILI. The large tidal volumes used are clearly not

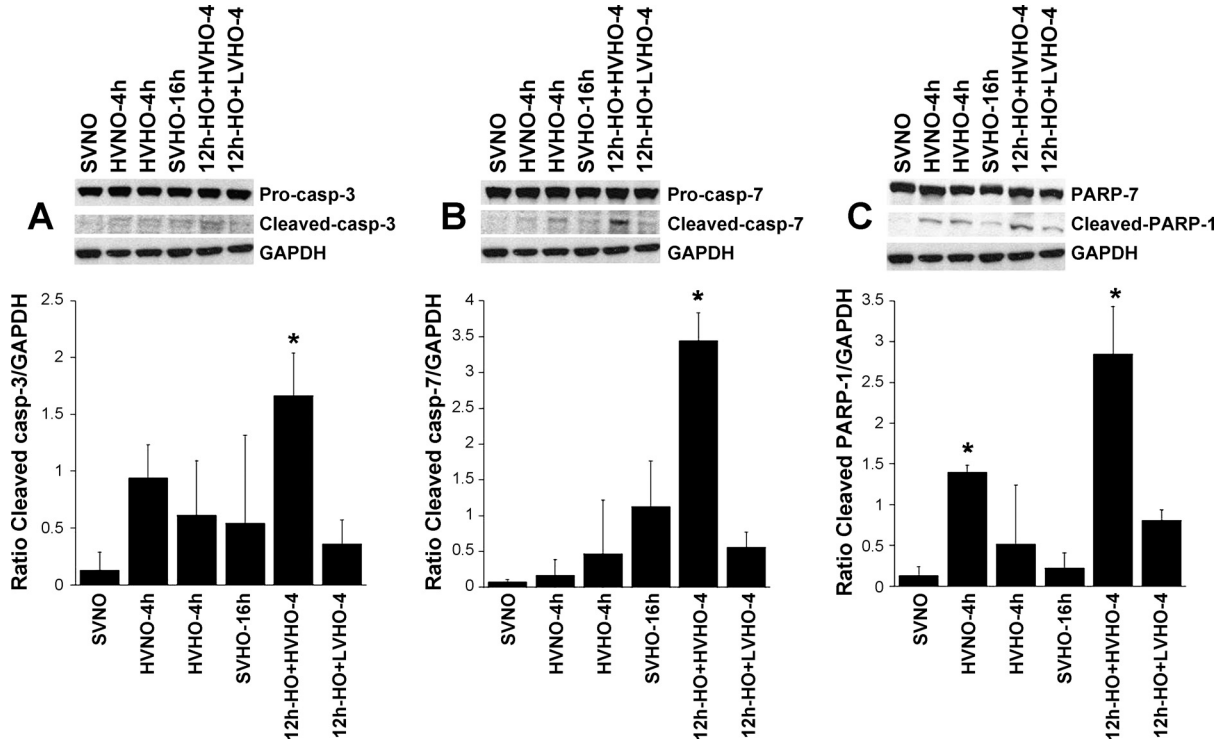

Fig. 7. Activation of executioner caspases, caspases-3 and -7, and their downstream substrate, PARP-1, in a mouse alveolar epithelial cell line (MLE-12) subjected to SVNO (static normoxia; *lane 1*), HVNO-4h (20% cyclic stretch normoxia; *lane 2*), HVHO-4h (20% cyclic stretch HO; *lane 3*), SVHO-16h (static HO; *lane 4*), 12h-HO+HVHO-4h (12-h static HO followed by 20% cyclic stretch HO; *lane 5*), and 12h-HO+LVHO-4h (12-h static HO followed by 6% cyclic stretch HO; *lane 6*) in Fig. 6, *A–C*. Increased caspase-3/7 cleavage was observed after 12h-HO+HVHO-4h (*$P < 0.05$), whereas significant PARP-1 cleavage was seen in HVNO-4h and 12h-HO+HVHO-4h conditions (*$P < 0.05$). All 3 blots from each set of experiments were developed on the same film. The blotting, development, and exposure conditions were the same for all 3 independent experiments. Representative blots are shown above the densitometry data from 3 independent experiments in which 4 wells were pooled for each condition.

clinically applicable, especially in light of the advantageous outcomes observed with low tidal volume ventilation in ARDS (1). It is also unlikely that a patient with ALI would be ventilated without the benefit of PEEP. We attempted to design this model to closely approximate what happens to patients who present with respiratory distress. This is what prompted the use of 12 h of exposure to HO before mechanical ventilation. However, the short duration of mechanical ventilation and the obvious species difference limits the applicability of our findings to the clinical setting.

The objective of this study was to test the hypothesis that the combined insults of HO and HV produce more severe lung injury than either insult alone and to determine whether preexposure to HO before initiation of mechanical ventilation increases the susceptibility to VILI. The possible reasons why HO or HV alone did not induce significant lung injury could be due to insufficient production of reactive oxygen species (ROS) and hence less oxidative damage occurred. Alternatively, even in the absence of direct oxidative damage to lung cells, the production of ROS with either individual insult alone was insufficient to alter oxidative signaling in such a way as to promote activation of cell death pathways. Another possibility is that neither of these conditions was implemented for a sufficient time to produce significant injury. Our data suggest that the 12-h preexposure to HO before initiation of HV is critical to the development of severe lung injury and activation of proapoptotic pathways in this model.

Our second objective was to evaluate whether the enhanced lung injury in 12h-HO+HVHO-2h and -4h was associated with activation of caspase-dependent apoptosis. Our data show that 12h-HO+HVHO-2h and -4h cleaved terminal caspases-3 and -7 and their downstream substrate, PARP-1. Our results suggest that 12h-HO+HVHO-4h-induced apoptosis is mediated by caspase-7 and, to a lesser extent, caspase-3. No other conditions were sufficient to produce significant activation of the terminal caspases or cleavage of PARP-1 in vivo. These data support the hypothesis that both HO preexposure and subsequent HVHO are required to activate caspase-mediated apoptosis and play a role in the development of severe lung injury.

Our next objective was to identify the upstream initiator caspases to ascertain whether the apoptotic pathways originated from death receptor-mediated (extrinsic) or mitochondrial-mediated (intrinsic) pathways. Both caspase-8 and -9 were cleaved in 12h-HO+HVHO-2h and -4h. Cleaved caspase-9 was more abundant in 12h-HO+HVHO-2h. This may be due to consumption of active caspase-9 used to cleave downstream caspases. We observed minor activation of caspase-9 in SVHO-16h, but this was not associated with measurable activation of terminal caspases or PARP-1 cleavage. No other conditions increased caspase-8 or -9 activation.

Given that our immunoblot experiments were performed using whole lung homogenates, it was not clear which cell population(s) were undergoing activation of the apoptotic machinery. We therefore performed immunohistochemical staining, using antibodies directed against cleaved caspase-3, of fixed lung sections. These studies revealed that the primary cell type undergoing apoptosis is alveolar epithelium. Furthermore, our in vitro experiments clearly recapitulated our in vivo findings. PARP-1 cleavage was observed in nearly all in vitro treatment groups, likely due to non-caspase-mediated cleavage of PARP-1 (11). These data support the hypothesis that the alveolar epithelium is at risk for apoptosis when subjected to conditions comparable with 12h-HO+HVHO-4h and strengthen our in vivo observations. This does not preclude the possibility that other cell types (endothelial or immune cells) are also undergoing injury or death under these experimental conditions.

In conclusion, our results revealed that preexposure to HO primed the lungs for injury caused by subsequent exposure to HV with HO. The combination of HO and HV is crucial and plays a pivotal role in inducing lung injury-mediated caspase activation and hence epithelial apoptosis. Although the current experimental design does not prove a causal link between apoptosis and the observed lung injury, epithelial apoptosis is known to contribute to ALI in several different experimental models (16, 18). Further studies are necessary to deduce what pathways are activated during HO preexposure that "prime" the lung for injury when subsequently subjected to HVHO.

ACKNOWLEDGMENTS

We thank Linda White for technical assistance with immunohistochemistry and Crystal Stanton and Dr. Anand Kulkarni for assistance with slide digitizer.

GRANTS

This study was funded by National Heart, Lung, and Blood Institute Grants HL-081297, HL-094366, and HL-75503.

DISCLOSURES

No conflicts of interest, financial or otherwise, are declared by the author(s).

REFERENCES

1. **The Acute Respiratory Distress Syndrome Network.** Ventilation with lower tidal volumes as compared with traditional tidal volumes for acute lung injury and the acute respiratory distress syndrome. The Acute Respiratory Distress Syndrome Network. *N Engl J Med* 342: 1301–1308, 2000.
2. **Altemeier WA, Sinclair SE.** Hyperoxia in the intensive care unit: why more is not always better. *Curr Opin Crit Care* 13: 73–78, 2007.
3. **Bailey TC, Martin EL, Zhao L, Veldhuizen RA.** High oxygen concentrations predispose mouse lungs to the deleterious effects of high stretch ventilation. *J Appl Physiol* 94: 975–982, 2003.
4. **Clerch LB, Baras AS, Massaro GD, Hoffman EP, Massaro D.** DNA microarray analysis of neonatal mouse lung connects regulation of KDR with dexamethasone-induced inhibition of alveolar formation. *Am J Physiol Lung Cell Mol Physiol* 286: L411–L419, 2004.
5. **Davis JM, Penney DP, Notter RH, Metlay L, Dickerson B, Shapiro DL.** Lung injury in the neonatal piglet caused by hyperoxia and mechanical ventilation. *J Appl Physiol* 67: 1007–1012, 1989.
6. **Dos Santos CC.** Hyperoxic acute lung injury and ventilator-induced/associated lung injury: new insights into intracellular signaling pathways. *Crit Care* 11: 126, 2007.
7. **Duan WR, Garner DS, Williams SD, Funckes-Shippy CL, Spath IS, Blomme EA.** Comparison of immunohistochemistry for activated caspase-3 and cleaved cytokeratin 18 with the TUNEL method for quantification of apoptosis in histological sections of PC-3 subcutaneous xenografts. *J Pathol* 199: 221–228, 2003.
8. **Ehlert CA, Truog WE, Thibeault DW, Garg U, Norberg M, Rezaiekhaligh M, Mabry S, Ekekezie II.** Hyperoxia and tidal volume: independent and combined effects on neonatal pulmonary inflammation. *Biol Neonate* 90: 89–97, 2006.
9. **Esteban A, Anzueto A, Frutos F, Alia I, Brochard L, Stewart TE, Benito S, Epstein SK, Apezteguia C, Nightingale P, Arroliga AC, Tobin MJ.** Characteristics and outcomes in adult patients receiving mechanical ventilation: a 28-day international study. *JAMA* 287: 345–355, 2002.
10. **Hammerschmidt S, Kuhn H, Grasenack T, Gessner C, Wirtz H.** Apoptosis and necrosis induced by cyclic mechanical stretching in alveolar type II cells. *Am J Respir Cell Mol Biol* 30: 396–402, 2004.

11. **Johnson DE.** Noncaspase proteases in apoptosis. *Leukemia* 14: 1695–1703, 2000.
12. **Le A, Damico R, Damarla M, Boueiz A, Pae HH, Skirball J, Hasan E, Peng X, Chesley A, Crow MT, Reddy SP, Tuder RM, Hassoun PM.** Alveolar cell apoptosis is dependent on p38 MAP kinase-mediated activation of xanthine oxidoreductase in ventilator-induced lung injury. *J Appl Physiol* 105: 1282–1290, 2008.
13. **Li LF, Liao SK, Ko YS, Lee CH, Quinn DA.** Hyperoxia increases ventilator-induced lung injury via mitogen-activated protein kinases: a prospective, controlled animal experiment. *Crit Care* 11: R25, 2007.
14. **Liu YY, Liao SK, Huang CC, Tsai YH, Quinn DA, Li LF.** Role for nuclear factor-kappaB in augmented lung injury because of interaction between hyperoxia and high stretch ventilation. *Transl Res* 154: 228–240, 2009.
15. **Mantell LL, Lee PJ.** Signal transduction pathways in hyperoxia-induced lung cell death. *Mol Genet Metab* 71: 359–370, 2000.
16. **Martin TR, Hagimoto N, Nakamura M, Matute-Bello G.** Apoptosis and epithelial injury in the lungs. *Proc Am Thorac Soc* 2: 214–220, 2005.
17. **Matthay MA, Bhattacharya S, Gaver D, Ware LB, Lim LH, Syrkina O, Eyal F, Hubmayr R.** Ventilator-induced lung injury: in vivo and in vitro mechanisms. *Am J Physiol Lung Cell Mol Physiol* 283: L678–L682, 2002.
18. **Matute-Bello G, Martin TR.** Science review: apoptosis in acute lung injury. *Crit Care* 7: 355–358, 2003.
19. **Nash G, Blennerhassett JB, Pontoppidan H.** Pulmonary lesions associated with oxygen therapy and artifical ventilation. *N Engl J Med* 276: 368–374, 1967.
20. **Pagano A, Barazzone-Argiroffo C.** Alveolar cell death in hyperoxia-induced lung injury. *Ann NY Acad Sci* 1010: 405–416, 2003.
21. **Parthasarathi K, Ichimura H, Monma E, Lindert J, Quadri S, Issekutz A, Bhattacharya J.** Connexin 43 mediates spread of Ca^{2+}-dependent proinflammatory responses in lung capillaries. *J Clin Invest* 116: 2193–2200, 2006.
22. **Quinn DA, Moufarrej RK, Volokhov A, Hales CA.** Interactions of lung stretch, hyperoxia, and MIP-2 production in ventilator-induced lung injury. *J Appl Physiol* 93: 517–525, 2002.
23. **Rubenfeld GD, Caldwell E, Peabody E, Weaver J, Martin DP, Neff M, Stern EJ, Hudson LD.** Incidence and outcomes of acute lung injury. *N Engl J Med* 353: 1685–1693, 2005.
24. **Salazar E, Knowles JH.** An analysis of pressure-volume characteristics of the lungs. *J Appl Physiol* 19: 97–104, 1964.
25. **Sinclair SE, Altemeier WA, Matute-Bello G, Chi EY.** Augmented lung injury due to interaction between hyperoxia and mechanical ventilation. *Crit Care Med* 32: 2496–2501, 2004.
26. **Tschumperlin DJ, Margulies SS.** Equibiaxial deformation-induced injury of alveolar epithelial cells in vitro. *Am J Physiol Lung Cell Mol Physiol* 275: L1173–L1183, 1998.